Crystal Structure of the Complex of Carboxypeptidase A with a Strongly Bound Phosphonate in a New Crystalline Form: Comparison with Structures of Other Complexes[†,‡]

Hidong Kim and William N. Lipscomb*
Gibbs Chemical Laboratory, Harvard University, Cambridge, Massachusetts 02138
Received December 28, 1989

ABSTRACT: *O*-[[(1*R*)-[[*N*-(Phenylmethoxycarbonyl)-L-alanyl]amino]ethyl]hydroxyphosphinyl]-L-3-phenyllacetate [ZAA^P(O)F], an analogue of (benzyloxycarbonyl)-Ala-Ala-Phe or (benzyloxycarbonyl)-Ala-Ala-phenyllactate, binds to carboxypeptidase A with great affinity (K_i = 3 pM). Similar phosphonates have been shown to be transition-state analogues of the CPA-catalyzed hydrolysis [Hanson, J. E., Kaplan, A. P., & Bartlett, P. A. (1989) *Biochemistry 28*, 6294–6305]. In the present study, the structure of the complex of this phosphonate with carboxypeptidase A has been determined by X-ray crystallography to a resolution of 2.0 Å. The complex crystallizes in the space group $P2_12_12_1$ with cell dimensions a = 61.9 Å, b = 67.2 Å, and c = 76.2 Å. The structure of the complex was solved by molecular replacement. Refinement of the structure against 20776 unique reflections between 10.0 and 2.0 Å yields a crystallographic residual of 0.193, including 140 water molecules. The two phosphinyl oxygens of the inhibitor bind to the active-site zinc at 2.2 Å on the electrophilic (Arg-127) side and 3.1 Å on the nucleophilic (Glu-270) side. Various features of the binding mode of this phosphonate inhibitor are consistent with the hypothesis that carboxypeptidase A catalyzed hydrolysis proceeds through a general-base mechanism in which the carbonyl carbon of the substrate is attacked by Zn–hydroxyl (or Zn–water). An unexpected feature of the bound inhibitor, the cis carbamoyl ester bond at the benzyloxycarbonyl linkage to alanine, allows the benzyloxycarbonyl phenyl ring of the inhibitor to interact favorably with Tyr-198. This complex structure is compared with previous structures of carboxypeptidase A, including the complexes with the potato inhibitor, a hydrated keto methylene substrate analogue, and a phosphonamidate inhibitor. Comparisons are also made with the complexes of thermolysin with some phosphonamidate inhibitors.

The three-dimensional structures of substrate-like inhibitors of bovine carboxypeptidase A (CPA;[1] EC 3.4.17.1) bound to CPA have provided a basis for mechanistic proposals for further studies by other methods (Christianson & Lipscomb, 1988a, 1989). This zinc protease hydrolyzes peptide or ester bonds at the C-terminus of the substrate. The elucidation of the mechanism of the CPA-catalyzed hydrolysis is a major focus of the study of this enzyme. The two plausible candidates for nucleophilic attack at the scissile carbonyl of the substrate in the hydrolysis reaction are either Zn–hydroxyl (the general-base mechanism) or Glu-270 (the acyl mechanism).

One structural approach in the mechanistic investigation of CPA has been the presentation to the enzyme of various compounds containing an intact carbonyl group at the bond analogous to the scissile bond of a substrate. Such analogues have included ketones, which are not appreciably hydrated in solution: 5-benzamido-2-benzyl-4-pentanoic acid (Christianson et al., 1987; Grobelny et al., 1985) and *N*-(*tert*-butoxycarbonyl)-5-amino-2-benzyl-4-oxo-6-phenylhexanoic acid (Shoham et al., 1988) (Figure 1). These ketones have a CH_2 group in place of the NH of a peptide bond or an O of an ester bond at the potential cleavage site. Both of these ketones are observed bound with the original carbonyl carbon converted to a tetrahedral carbon either by the Zn–hydroxyl unit or with the very small percentage, 0.2% or less, of the tetrahedral hydrated form selectively bound by the enzyme. These structures resemble the tetrahedral intermediate expected in the general-base mechanism, and not that expected in the acyl mechanism involving nucleophilic attack by Glu-270 (Figure 2). From these studies, we can at least conclude that the enzyme prefers to select the hydrated ketones or convert these ketones to the tetrahedral form rather than follow the acyl pathway.

A second structural approach has been the study of the binding of inhibitors with preformed tetrahedral centers such as the hydrated forms of 2-benzyl-3-formylpropanoic acid (Christianson & Lipscomb, 1985; Galardy & Kortylewicz, 1984) and 2-benzyl-4-oxo-5,5,5-trifluoropentanoic acid (Christianson & Lipscomb, 1986; Gelb et al., 1985) (Figure 1). In these two examples, the enzyme showed a preference for selection of (or conversion to) the tetrahedral form, rather than binding the unhydrated form or reacting to form the covalent acyl adduct. The fully formed tetrahedral phosphonamidate inhibitor *N*-[[[(benzyloxycarbonyl)amino]-methyl]hydroxyphosphinyl]-L-phenylalanine has also been subjected to structural study (Christianson & Lipscomb, 1988b; Jacobsen & Bartlett, 1981) (Figure 1). Like the other two inhibitors, it binds to CPA with the two oxygens of its tetrahedral phosphorus coordinated to zinc, and one of these

[†] Support for this research was provided by a National Science Foundation Predoctoral Fellowship to H.K. and a grant (GM-06920) to W.N.L. from the National Institutes of Health.

[‡] Crystallographic coordinates of carboxypeptidase A/ZAA^P(O)F have been deposited into the Brookhaven Protein Data Bank under entry name 6CPA coordinates.

[1] Abbreviations: CPA, carboxypeptidase A; ZAA^P(O)F, strongly bound phosphonate inhibitor of CPA *O*-[[(1*R*)-[[*N*-(phenylmethoxycarbonyl)-L-alanyl]amino]ethyl]hydroxyphosphinyl]-L-3-phenyllactate; TLN, thermolysin; ZGP′, the dipeptide analogue phosphonamidate inhibitor of CPA *N*-[[[(benzyloxycarbonyl)amino]methyl]hydroxyphosphinyl]-L-phenylalanine; ZG^{P}LL, phosphonamidate inhibitor of TLN Cbz-Gly^P-L-Leu-L-Leu; ZF^{P}LA, phosphonamidate inhibitor of TLN Cbz-Phe^P-L-Leu-L-Ala; rms, root mean square; F_o and F_c, observed and calculated structure factors.

0006-2960/90/0429-5546$02.50/0

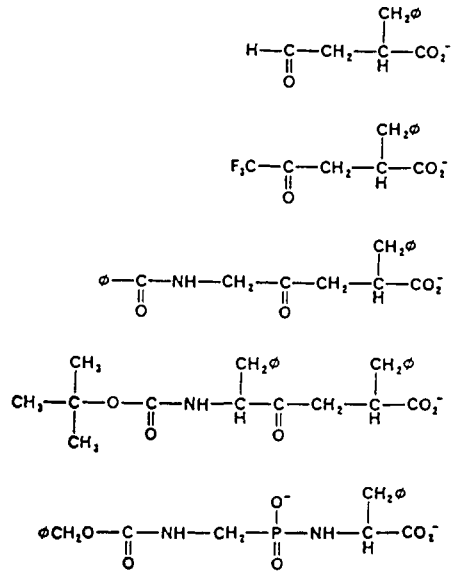

FIGURE 1: CPA inhibitors. From top to bottom: 2-benzyl-4-formylpropanoic acid, $K_i = 4.8 \times 10^{-7}$ M (enantiomeric mixture); 2-benzyl-4-oxo-5,5,5-trifluoropentanoic acid, $K_i = 2 \times 10^{-7}$ M (enantiomeric mixture); 5-benzamido-2-benzyl-4-oxopentanoic acid, $K_i = 4.8 \times 10^{-5}$ M (enantiomeric mixture); 5-amino-*N*-(*tert*-butoxycarbonyl)-2-benzyl-4-oxo-6-phenylhexanoic acid, $K_i = 6.7 \times 10^{-7}$ M (diastereomeric mixture); *N*-[[[(benzyloxycarbonyl)amino]methyl]-hydroxyphosphinyl]-L-phenylalanine, $K_i = 9 \times 10^{-8}$ M. Reproduced with permission from Christianson and Lipscomb (1988a). Copyright 1988 Springer.

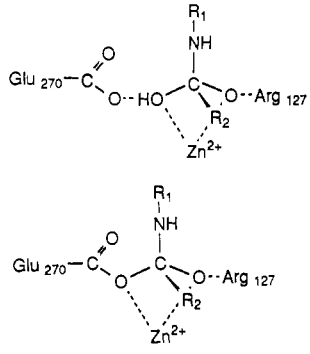

FIGURE 2: Tetrahedral carbon intermediates formed in the general-base (top) and acyl (bottom) mechanisms for CPA-catalyzed hydrolysis. Covalent bonds are represented by solid lines and hydrogen bonds are represented by dashed lines.

oxygens closely interacting with Arg-127. These results are models of the tetrahedral intermediate in the general-base mechanism for CPA-catalyzed hydrolysis of peptides and esters. However, in the absence of further information, the binding of a preformed tetrahedral intermediate does not provide a basis for determining the mechanism.

Here, we examine the X-ray crystal structure of the complex of CPA with a very strongly bound phosphonate inhibitor. The inhibitor, *O*-[[(1*R*)-[[*N*-(phenylmethoxycarbonyl)-L-alanyl]-amino]ethyl]hydroxphosphinyl]-L-3-phenyllactate (Figure 3), with a K_i of 3 pM, is an analogue of the substrates Cbz-Ala-Ala-Phe or Cbz-Ala-Ala-phenyllactate (Hanson et al., 1989). The binding mode of this inhibitor is taken to be a model of an intermediate state along the reaction pathway of the CPA-catalyzed hydrolysis. We emphasize that this structural study alone cannot be used to determine the mechanism. The information that does allow mechanistic proposals from this study are the relationships between structure and binding affinity for this and other phosphonate inhibitors of CPA. The correlation between the K_i's of several phosphonate inhibitors and the K_m/k_{cat}'s of the corresponding

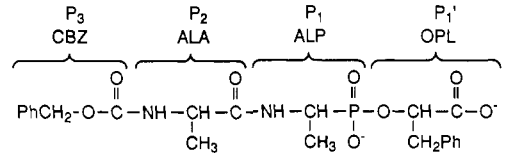

FIGURE 3: Extremely tight-binding phosphonate inhibitor of CPA, *O*-[[(1*R*)-[[*N*-(phenylmethoxycarbonyl)-L-alanyl]amino]ethyl]-hydroxyphosphinyl]-L-3-phenyllactate [ZAA^P(O)F], $K_i = 3$ pM. The four residual portions of the inhibitor are indicated. In a true substrate, hydrolysis occurs at the P_1'–P_1 linkage. CBZ, benzyloxycarbonyl; ALA, alanine; ALP = alanine^P; OPL, (O)phenylalanine.

Table I: Data Intensity Statistics by Resolution Shell

			cumulative percentages			
res (Å)	no. of refl	R_{merge}	$I \le 1\sigma$	$I \le 2\sigma$	$I \le 3\sigma$	$I > 3\sigma$
7.52	468	0.048	0.4	1.1	1.7	98.3
5.40	748	0.028	0.1	0.3	0.5	99.5
4.43	932	0.028	0.2	0.3	0.6	99.4
3.85	1097	0.030	0.0	0.2	0.5	99.5
3.45	1228	0.033	0.4	0.8	1.1	98.9
3.15	1324	0.039	0.4	0.8	1.7	98.3
2.92	1448	0.045	0.3	0.9	2.1	97.9
2.73	1558	0.051	0.7	2.0	3.3	96.7
2.58	1630	0.057	0.9	2.7	4.4	95.6
2.45	1733	0.062	1.1	2.7	4.7	95.3
2.33	1808	0.066	1.3	3.7	5.6	94.4
2.23	1875	0.071	1.7	4.5	7.9	92.1
2.15	1978	0.077	2.8	5.8	9.9	90.1
2.07	1981	0.084	3.2	6.7	11.0	89.0
2.00	1988	0.080	5.7	12.9	19.5	80.5
overall	21796	0.043	1.6	3.8	6.2	93.8

peptide substrates supports the reaction pathway in which the tetrahedral intermediate is formed by the general-base mechanism (Hanson et al., 1989). In the present study, we provide a structural basis for this mechanistic conclusion, as well as for the tight-binding nature of the inhibitor.

Experimental Procedures

Bovine pancreatic CPA (type I) was purchased from Sigma and used without further purification. A 100% molar excess of ZAA^P(O)F was dissolved in this CPA suspension and solubilized to 15 mg/mL CPA with 1.2 M LiCl/0.02 M Tris (pH 7.4). After being dialyzed against 0.25 M LiCl/0.02 M Tris (pH 7.4) at 4 °C, the enzyme–inhibitor solution was filtered through a Millipore Millex-GV filter. Cocrystals were grown at room temperature from this filtered solution by the method of hanging drop vapor diffusion with 6% poly(ethylene glycol) 8000 as the precipitant. Within 1 week, crystals with an octahedral habit and edge lengths of 0.3 mm appeared. Precession photographs identified the space group as $P2_12_12_1$ with unit cell parameters $a = 61.9$ Å, $b = 67.2$ Å, and $c = 76.2$ Å and one molecule of complex per asymmetric unit. This is a new crystal form for CPA.

The X-ray diffraction data were collected at room temperature on a Siemens X-100A multiwire area detector equipped with Charles Supper double X-ray focusing mirrors by the oscillation method. Cu Kα radiation was produced by an Elliott GX-6 rotating anode X-ray generator. A total of 113639 reflections to 2.0 Å, of which 21796 are unique (99% completeness), was recorded from four crystals. The 20776 unique reflections (95% completeness) between 10.0 and 2.0 Å with intensity greater than 2σ were used in the refinement. The merging R ($R_{merge} = \sum_{hkl} \sum_i |I - \bar{I}| / \sum_i I$) for the data was 0.043. See Table I for details.

The CCP4 molecular replacement package (Machin, 1985) was used to determine the structure of the complex in this new orthorhombic crystal form. The backbone of the native CPA structure in the $P2_1$ crystal form (Rees et al., 1983) was used

as the model probe. Rotation of this model (placed in a 200 Å × 200 Å × 200 Å P1 cell) against the data of the complex from 8.0 to 5.0 Å using the Crowther fast rotation function revealed a 5.3σ peak, which stood out clearly from all other peaks. The solution was $\alpha = 265.0°$, $\beta = 40.0°$, $\gamma = 5.0°$ (Daresbury convention). After application of this rotational solution, the model was placed in the cell by a full translational R_{factor} search. Using an 0.6-Å grid spacing, the search gave a 7.3σ solution for data from 7.0 to 6.0 Å, which was the highest peak on the search map. After the backbone model was rotated and translated according to the molecular replacement solution, side chains were added and the resulting model was subjected to rigid body refinement by X-PLOR (Brünger, 1988). After eight cycles of rigid body refinement, the crystallographic residual [$R_{factor} = \sum_{hkl}(||F_o| - |F_c||)/|F_o|$] dropped from 0.39 to 0.32 against data to 2.6 Å. Powell minimization refinement by X-PLOR further reduced the R_{factor} to 0.27. Addition of the active-site zinc to the model improved the R_{factor} to 0.26 after additional Powell minimization. At this point, the difference map of the structure ($F_{complex} - F_{nat,calc}$) clearly showed the electron density of the inhibitor in the active site and the side chain of active-site residue Tyr-248 in the "down" position, close to the inhibitor. The side chain of Tyr-248 was modeled into the down position and the enzyme including the active-site zinc was refined against data from 10.0 to 2.0 Å by simulated annealing (Brünger et al., 1987) to an R_{factor} of 0.25.

Initial coordinates for the inhibitor were determined by positioning the inhibitor into the active-site density of the $F_{complex} - F_{nat,calc}$ map, using the graphics program FRODO (Jones, 1982) on an Evans and Sutherland PS300, interfaced to a VAX 11/780. Water molecules were also placed in the structure according to the difference map, and the entire complex structure including 140 water molecules was refined by Powell minimization. Temperature factor refinement gave a final R_{factor} of 0.193. Throughout the refinement, all model building was done on an Evans and Sutherland PS300 using the graphics program FRODO. The final refined complex has rms deviations from ideal bond length and ideal bond angle of 0.012 Å and 2.8°, respectively. All rigid-body, simulated annealing, and Powell minimization refinements were executed with X-PLOR on a DECstation 3100. The coordinates of the complex are deposited in the Brookhaven Protein Data Bank.

Results

One molecule of intact ZAA^P(O)F occupies the active site of CPA. Occupancies of the S_1', S_1, and S_2 subsites of the primary binding groove by the corresponding inhibitor residues are clearly seen in the structure, as evidenced by the $F_o - F_c$ map of the refined complex for which the coordinates of the inhibitor were omitted from the structure factor calculations (Figure 4). These three subsites bind ZAA^P(O)F as they did previously studied complexes, particularly those involving two extended ligands: the potato inhibitor (Rees & Lipscomb, 1982) and a hydrated keto methylene substrate analogue (Shoham et al., 1988).

The side chain of the P_1' phenylalanine occupies the hydrophobic pocket of the S_1' subsite. Its terminal carboxylate makes hydrogen bond contacts to the side chains of Asn-144, Arg-145, Tyr-248, and Arg-127. The phosphinyl group of the inhibitor is coordinated to the zinc. Looking down the active-site cleft from the amino end of the inhibitor to the carboxyl end, on the "electrophilic" side of the zinc coordination sphere, we see that one phosphinyl oxygen is bound by Arg-127 and, on the "nucleophilic" side, that the other phosphinyl oxygen is bound by Glu-270 (Figure 7). Unlike the structure of the CPA–phosphonamidate complex (Christianson & Lipscomb, 1988b), the phosphinyl group is rotated toward Arg-127 instead of Glu-270. The side chain of the P_1 alanine juts into the hydrophobic cavity of subsite S_1. The phenolic side chain of enzyme residue Tyr-248 is in the characteristic "down" position for bound ligands. In the present complex, the phenolic oxygen accepts a hydrogen bond from the amide NH group of the P_1 portion of the inhibitor. The P_2 alanine residue rests in the S_2 subsite with its carbonyl oxygen bound by Arg-71.

Table II: Selected CPA–ZAA^P(O)F Interactions[a]

enzyme atom	inhibitor atom	distance (Å)
Arg-145 $N_\eta 1$	carboxylate O1	2.4*
Arg-145 $N_\eta 1$	carboxylate O2	2.9*
Arg-145 $N_\eta 2$	carboxylate O2	3.3*
Asn-144 $N_\delta 2$	carboxylate O1	2.8*
Glu-270 $O_\epsilon 1$	phosphinyl O2	3.3
Glu-270 $O_\epsilon 2$	phosphinyl O2	2.2*
Ser-197 O	phosphinyl O2	3.2
Arg-127 $N_\eta 1$	carboxylate O2	3.0*
Arg-127 $N_\eta 2$	phosphinyl O1	2.8*
Arg-127 $N_\eta 2$	alanine O	3.0*
Tyr-248 phenolic O	(O)phenylalanine O	3.3
Tyr-248 phenolic O	alanine^P N	3.1*
Arg-71 $N_\eta 1$	alanine O	3.0*
Zn	phosphinyl O2	3.1
Zn	phosphinyl O1	2.2

[a] Presumed hydrogen bonds are denoted by an asterisk.

Neither the carbonyl nor the benzyl oxygen of the Cbz portion of ZAA^P(O)F is within hydrogen-bonding distance of any atoms of the enzyme. However, a stabilizing enzyme–inhibitor interaction seen in this region is an edge-to-face interaction between the phenyl ring of the Cbz moiety and the phenol ring of Tyr-198. In order to achieve this interaction, the carbamoyl ester linkage between the P_2 alanine and the Cbz is in the unexpected cis conformation, as unequivocally revealed by the $F_o - F_c$ density (Figure 5). Inhibitor–enzyme distances are given in Table II.

The enzyme itself shows no significant changes in its conformation from that of the native enzyme in the $P2_1$ crystal form (Rees et al., 1983) except for the rotation about the C_α–C_β bond of Tyr-248 and movement of the associated strand of β-structure, both of which have been seen in the structures of all CPA–ligand complexes. After superposition of the backbone of the present complex on the backbone of native CPA by X-PLOR, the rms deviation in position for backbone atoms is 0.34 Å and for all atoms is 0.86 Å. Besides the region around Tyr-248, the largest deviations from the native structure are seen in residues 133–135 and 210–211, where some backbone atoms have moved up to 1.1 Å from the native structure. Similar deviations were seen in residues 133–135 in the potato inhibitor complex (Rees & Lipscomb, 1982). These residues are at the "tip" of the conical CPA molecule, near the Cys-138–Cys-161 disulfide bridge. This is a region of the enzyme that is very much exposed to solvent. The electron density in this region is weak and so these atomic coordinates are probably less accurate than for the rest of the enzyme. In contrast to the electron density for residues 133–135, the electron density of residues 210–211 is quite strong and we are confident of the accuracy of these coordinates. These residues are involved in intermolecular contacts in both the present complex and the native structure, albeit involving different contact residues in each case. (An atom is considered to make an intermolecular contact if it is within 4 Å of any atoms of a symmetry-related complex.) A difference between the present complex and the native enzyme seen near this region is that the phenolic oxygen of Tyr-208

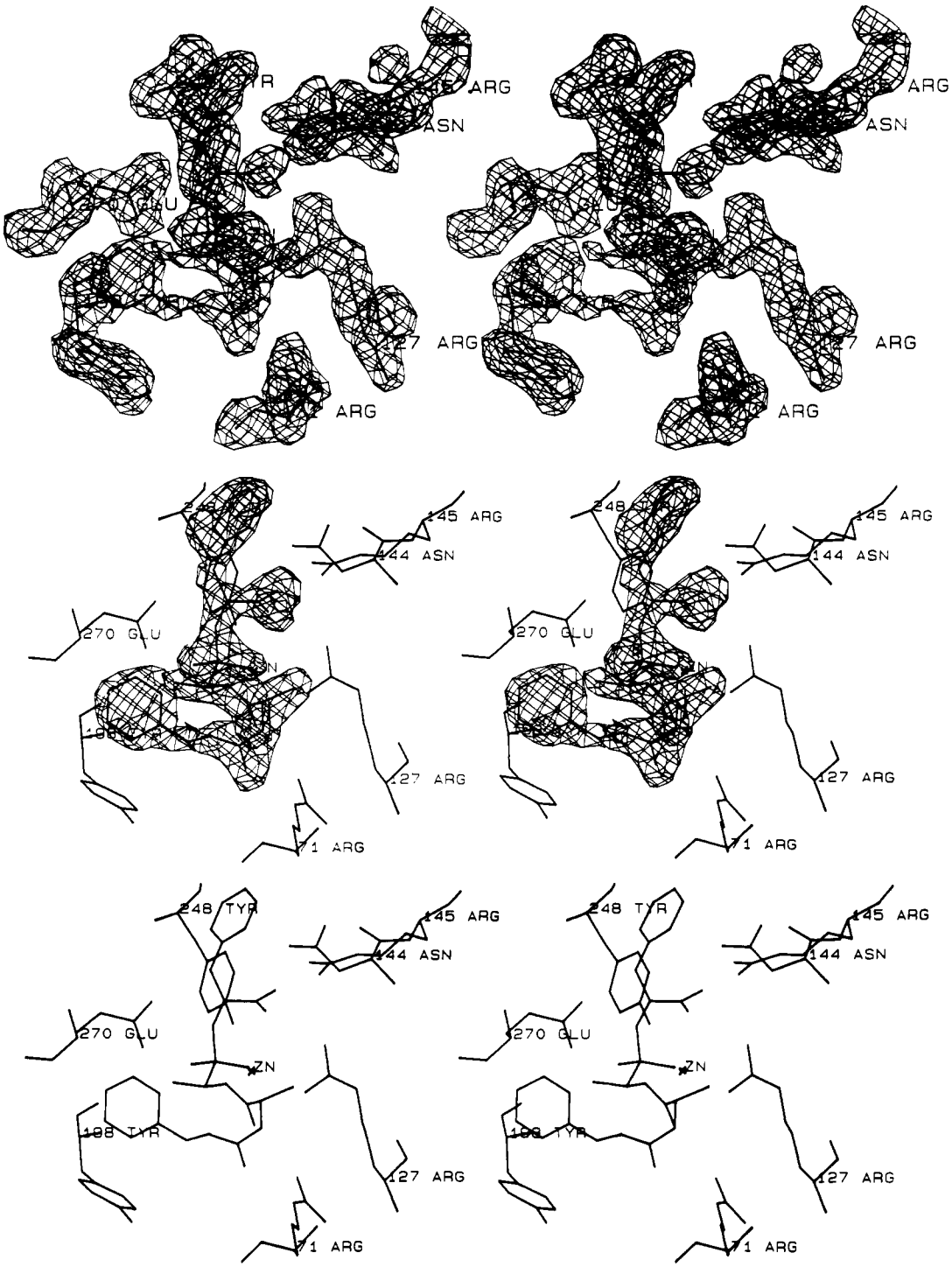

FIGURE 4: (Top) $F_o - F_c$ map in which $ZAA^P(O)F$, the zinc, Arg-71, Arg-127, Asn-144, Arg-145, Tyr-198, Tyr-248, and Glu-270 were omitted from the structure factor calculation. The contour level is 2.8σ. Enzyme–inhibitor interactions are clearly seen from this map. The coordinates of the final refined complex are superimposed on the density. (Middle) The same view of the active site as in (top). The density is from an $F_o - F_c$ map in which $ZAA^P(O)F$ was omitted from the structure factor calculation. The contour level is 3.2σ. (Bottom) The coordinates of the inhibitor and the key active-site residues in the final refined complex.

in the present complex makes an intermolecular contact with the carbonyl oxygen of Leu-233 and the side chain of Tyr-234 in a symmetry-related complex molecule. In the native structure, Tyr-208 makes no intermolecular contacts. At the active site, with the exception of Tyr-248, there are no significant conformational deviations from the native structure. In the present complex, the phenolic oxygen of Tyr-198 makes a contact with $N_\eta 2$ of Arg-40 of a symmetry-related complex. Tyr-198 in the native structure also makes intermolecular contacts near this region. For $ZAA^P(O)F$, only its Cbz portion is sufficiently exposed to make intermolecular contacts. Its carbonyl and benzyl oxygens make no intermolecular contacts, but the phenyl ring does interact with the side chain of Arg-45 from a neighboring molecule. The present study marks the third different crystalline form of CPA whose structure has been solved (Quiocho & Lipscomb, 1971; Rees & Lipscomb, 1982;). That there are no gross conformational differences in the enzyme among these three different crystal forms indicates that crystal-packing forces in these structures impose little influence on the tertiary structure of CPA. The present study increases our confidence that the conformations seen in the crystal structure are those which exist in solution.

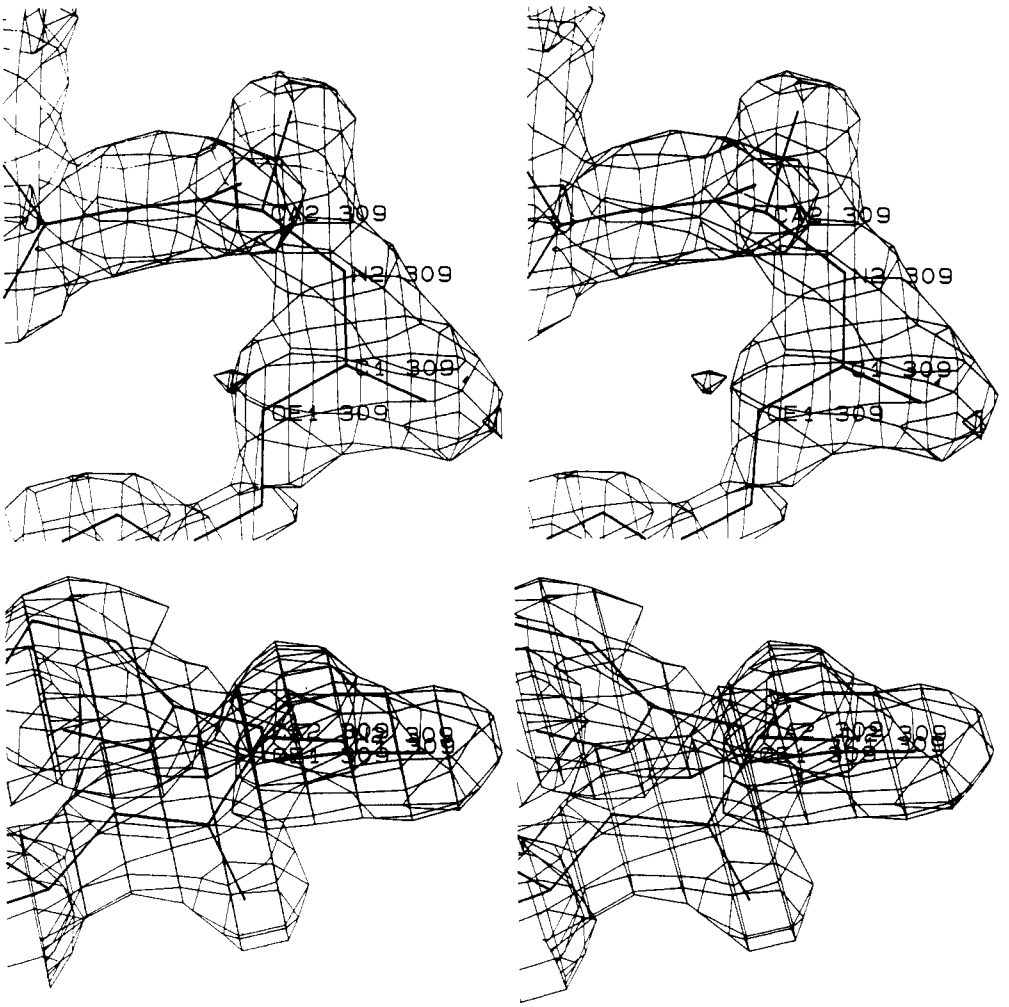

FIGURE 5: Electron density at the carbamoyl ester linkage between the P_3 and P_2 portions of $ZAA^P(O)F$. Fourier coefficients and phases are the same as the ones in Figure 4 (middle) and the coordinates of the the inhibitor from the final refined complex are superimposed. The two views shown are approximately perpendicular to each other. The carbamoyl ester bond is clearly i the cis conformation. ["309" is the residue designation for $ZAA^P(O)F$ in the coordinate file.]

The coordination sphere about the zinc due to enzyme ligands is essentially unchanged from the native structure. The salient feature is that coordination by the side-chain carboxylate of Glu-72 remains bidentate. The coordination of the phosphinyl oxygens of $ZAA^P(O)F$ to the zinc is unidentate and the zinc is 0.4 Å out of the plane of the phosphinyl group. These features are expected since phosphinyl–metal interactions are predominantly unidentate and noncoplanar (Alexander et al., 1990). This unidentate coordination is similar to that seen in the complexes of phosphonamidates with thermolysin in which the phosphinyl oxygen bound to the active-site electrophile was closer to the zinc than was the other phosphinyl oxygen (Tronrud et al., 1986; Holden et al., 1987). See Table III for details of the coordination sphere about zinc.

Table III: Zinc Coordination

ligand	distance (Å)
His-69 $N_\delta 1$	2.1
His-196 $N_\delta 1$	2.2
Glu-72 $O_\epsilon 1$	2.2
Glu-72 $O_\epsilon 2$	2.3
phosphinyl O1	2.2
phosphinyl O2	3.1

Discussion

Binding of the Inhibitor. The most interesting aspect of the present CPA–inhibitor complex is the extremely tight binding nature of the inhibitor. $ZAA^P(O)F$ is one of a series of noncovalent tight-binding phosphonate transition-state analogues of CPA whose properties of inhibition have been recently examined by Bartlett and co-workers (Hanson et al., 1989). $ZAA^P(O)F$ is one of three phosphonate inhibitors with dissociation constants less than 5 pM. These phosphonates bind to the enzyme more strongly by 3 orders of magnitude than any other reported CPA inhibitor. Moreover, these CPA–inhibitor complexes show among the very strongest enzyme–ligand interactions known. Previously, the CPA–inhibitor complex with the strongest binding constant studied by X-ray crystallography was the CPA–potato inhibitor complex with a K_i of 5 nM (Rees & Lipscomb, 1982). This 39 amino acid inhibitor was able to bind so tightly to the enzyme due to the many contacts that it made to the enzyme, 43 polar and nonpolar in all, about 3 times more than the number of contacts seen in a typical dipeptide analogue CPA inhibitor with a K_i in the millimolar to micromolar range. This "better binding through more contacts" explanation is certainly not applicable in the case of $ZAA^P(O)F$, in the sense that there are far fewer enzyme–inhibitor contacts for $ZAA^P(O)F$ than for the potato inhibitor and yet the binding is much stronger for $ZAA^P(O)F$.

One of the explanations for the strength of binding in the present case likely lies in transition-state-binding theory (Pauling, 1948; Leinhard, 1973; Wolfenden, 1976). According to this theory, an enzyme binds the substrate(s) of its catalytic reaction most tightly at the "transition state" of the reaction.[2]

Therefore, the more closely a ligand resembles the transition state of the reaction, the stronger should be its binding constant. Leinhard proposed that the dissociation constant for an enzyme–transition-state complex should be on the order of femtomolar (Leinhard, 1973). Although not femtomolar, the 3 pM dissociation constant for $ZAA^P(O)F$ would appear to make it a good transition-state analogue and, at least, the best transition-state analogue of the CPA-catalyzed reaction studied thus far. However, tight binding is neither a necessary nor a sufficient condition for transition-state analogy. An additional criterion for transition-state analogy is that substituent effects on the K_i's of a series of putative transition-state-analogue inhibitors correlate with the same substituent effects on the K_m/k_{cat}'s of the corresponding substrates (Thompson, 1973). Using this criterion, Bartlett and coworkers have indeed demonstrated transition-state analogy for a series of phosphonate analogues of tri- and tetrapeptide substrates (Hanson et al., 1989). If the binding mode of $ZAA^P(O)F$ is taken as an analogue of the transition state of the CPA-catalyzed hydrolysis, the phosphonate moiety of $ZAA^P(O)F$ is a model for a noncovalent tetrahedral intermediate formed via the general-base mechanism (Figure 2). Invoking transition-state-binding theory to partially explain the strong binding of this inhibitor emphasizes the interaction between the enzyme and the characteristic transition-state-mimicking moiety, which in the present case is the tetrahedral phosphonate and, specifically, the two phosphinyl oxygens. These two oxygens are coordinated to the active-site zinc, to Glu-270, and to Arg-127, which are three crucial residues in the proposed general-base mechanism for CPA-catalyzed hydrolysis (Figure 8). Under the hypothesis of the general-base mechanism, the binding of the phosphinyl moiety is a model for the tetrahedral *gem*-diolate that arises from the attack by a water molecule, activated by the zinc and Glu-270, on the scissile carbonyl which has been polarized by Arg-127.

In addition to enzyme–inhibitor interactions highlighted by transition-state-binding theory, interactions in the CPA-$ZAA^P(O)F$ complex other than those at the phosphonate moiety must also be partly responsible for the extremely tight binding nature of this complex. The terminal carboxylate of the inhibitor is bound by Arg-145, Asn-144, and Tyr-248. These three residues appear to provide specificity for substrates bearing a free terminal carboxylate (Christianson & Lipscomb, 1988b). Tyr-248 also provides further binding specificity for substrates with penultimate peptide bonds by accepting a hydrogen bond from the amide group of the P_1 portion of the substrate. Moving further down the inhibitor, away from the phosphonate moiety, the carbonyl oxygen of the P_2 alanine makes a contact with the the guanidinium group of Arg-71. These hydrogen-bonding interactions were also seen in the complexes of CPA with the potato inhibitor (Rees & Lipscomb, 1982) and a hydrated keto methylene substrate analogue (Shoham et al., 1988).

The hydrogen-bonding interactions cited here well define the first three subsites of the primary binding groove. The effects of substrate length on the kinetics of peptide hydrolysis show that the active-site binding groove comprises five binding subsites (Abramowitz et al., 1967). Of the CPA complexes studied thus far, only the one involving the 39 amino acid potato inhibitor had a ligand that might have been long enough to occupy all five putative subsites. However, the P_3 residue (a proline) made only a weak interaction with the enzyme and no evidence for a fifth subsite, S_4, was seen. In the hydrated keto methylene substrate analogue complex, the Arg-71 hydrogen-bonding interaction of subsite S_2 involved the carbonyl oxygen of the *tert*-butoxycarbonyl protecting group of the inhibitor and not an actual amino acid residue (Shoham et al., 1988). The carbonyl of the Cbz protecting group of $ZAA^P(O)F$ was similarly expected to make a strong polar interaction with the enzyme, thereby indicating the S_3 subsite. This expectation was not realized as neither the carbonyl oxygen nor the benzyl oxygen of the Cbz group is within hydrogen-bonding distance of any atoms of the enzyme. Beyond its P_2 portion a substrate would be mainly in solvent unless it were to bend back toward itself in order to maintain its contacts with the enzyme. This type of bending behavior is dramatically seen in the binding mode of $ZAA^P(O)F$. The cis conformation of its carbamoyl ester linkage between its Cbz and P_2 portions imposes a sharp bend in the molecule, allowing the phenyl ring of Cbz to interact favorably with Tyr-198. This cis carbamoyl ester bond may also affect the kinetics of the binding, which will be discussed later.

Although hydrogen-bonding interactions have been stressed thus far, the importance of van der Waals and other weaker interactions in the binding of this substrate cannot be overlooked. The phenylalanine side chain of the P_1' portion occupies the hydrophobic pocket of the S_1' subsite as expected. This hydrophobic pocket allows preference of CPA for substrates with aromatic and branched-chain C-terminal amino acid residues (Hanson et al., 1989). The alanine side chains of the P_1 and P_2 portions jut into the hydrophobic cavities of the S_1 and S_2 subsites, respectively. Similar enzyme–inhibitor interactions at the S_1 subsite were also seen in the complexes of CPA with the potato inhibitor (Rees & Lipscomb, 1982) and a hydrated keto methylene substrate analogue (Shoham et al., 1988), involving valine and phenylalanine side chains, respectively. At the far end of $ZAA^P(O)F$, the phenyl ring of the Cbz portion makes a favorable edge-to-face interaction with the phenol ring of Tyr-198. Aromatic edge-to-face interactions have been detailed by Burley and Petsko, and according to their convention, the centers of the Cbz phenyl and Tyr-198 phenol rings are 5.8 Å apart, θ is 38°, and the interplanar angle is 90° (Burley & Petsko, 1985, 1986). If the Cbz group is replaced with a dansyl group, the resulting inhibitor binds less tightly by nearly an order of magnitude (Hanson et al., 1989). Although an aromatic–aromatic interaction is possible with the dansyl inhibitor, the optimization of such an interaction in $ZAA^P(O)F$ may contribute significantly to the tighter binding of the Cbz inhibitor. Such edge-to-face interactions involving Tyr-198 have been seen in the complexes of CPA with the hydrated keto methylene substrate analogue and the phosphonamidate and in some complexes of thermolysin, involving Phe-114 of thermolysin (Kester & Matthews, 1977; Monzingo & Matthews, 1984; Holden et al., 1987). What sets the edge-to-face interaction of the present study apart from the others is that accompanying this interaction there is an unexpected conformational feature in the bound inhibitor, namely, the cis carbamoyl ester linkage between the P_3 and P_2 portions. Since there are no hydrogen-bonding interactions between the inhibitor and the enzyme involving the Cbz portion, this edge-to-face interaction seems to be important in securing the bound inhibitor in its particular conformation.

Mechanism of Hydrolysis. Structural studies of the binding of $ZAA^P(O)F$ and all inhibitors with preformed tetrahedral centers cannot be used as a test for determining the mechanism of CPA-catalyzed hydrolysis. Presenting the enzyme a pre-

[2] It may be sufficient that binding of the enzyme to some species along the reaction pathway is enhanced over binding of the enzyme to the substrate.

Table IV: Phosphinyl Oxygen–Zinc Interactions[a] (Å)

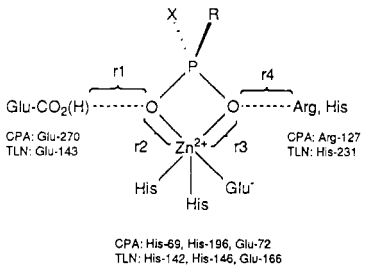

enzyme	inhibitor	X	*r*1	*r*2	*r*3	*r*4	reference
CPA	ZGP′	NHR′	2.6	2.4	3.5	2.6	Christianson & Lipscomb, 1988b
CPA	ZAA^P(O)F	OR′	2.2	3.1	2.2	2.9	this work
TLN	phosphoramidon	NHR′	2.5	3.4	1.8	3.2	Tronrud et al., 1986
TLN	ZG^{P}LL	NHR′	2.5	3.0	2.1	2.9	Holden et al., 1987
TLN	ZF^{P}LA	NHR′	2.3	2.6	2.2	2.7	Holden et al., 1987

[a] After Christianson and Lipscomb (1988b).

formed tetrahedral center precludes the formation of a covalent acylenzyme adduct, if indeed the acyl pathway is the mechanism for hydrolysis. However, the binding modes of ZAA^P(O)F and the other CPA complexes involving inhibitors with preformed tetrahedral centers (Christianson & Lipscomb, 1985, 1986, 1988b) are consistent with the hypothesis that the general-base mechanism is the preferred mechanism for hydrolysis. The salient structural features are coordination of the *gem*-diolate or phosphinyl moiety to the zinc and/or Arg-127 and a short distance between a diolate or phosphinyl oxygen and a glutamate oxygen of Glu-270. The hypothesis of the general-base mechanism seems justified by the structural studies of CPA in which the enzyme either hydrated or preferentially bound hydrated ketonic substrate analogues (Christianson et al., 1987; Shoham et al., 1988) and the study of Bartlett, which demonstrated the transition-state analogy for phosphonate inhibitors of CPA (Hanson et al., 1989). The results of Barlett's study strongly support the general-base mechanism over the acyl mechanism for the analogous substrates of the phosphonates that were examined. The covalent tetrahedral intermediate formed in the acyl mechanism could not be effectively modeled by such phosphonates.

Further evidence that the binding of ZAA^P(O)F is consistent with, if not supportive of, the general-base mechanism is the comparison of the present complex with complexes of thermolysin. Thermolysin (TLN) is a zinc endoprotease with a similar arrangement of active-site catalytic residues (Holmes & Matthews, 1982). The general-base mechanism is firmly accepted for the TLN-catalyzed hydrolysis (Matthews, 1988). Crystal structures of the complexes of several phosphinyl inhibitors of TLN with TLN have been reported by Matthews and co-workers (Holden et al., 1987; Tronrud et al., 1986). In three phosphinyl inhibitors of TLN, phosphoramidon, ZG^{P}LL, and ZF^{P}LA (Figure 6), with K_i's 28, 9.1, and 0.068 nM, respectively, (Bartlett & Marlowe, 1983, 1987a), there is a definite trend in the coordination of the two phosphinyl oxygens to the zinc. Specifically, as the K_i of the inhibitor decreases, the coordination of the phosphinyl oxygens gradually rotates toward the nucleophilic active-site residue (Glu-143) and the Zn–phosphinyl oxygen distances become nearly bidentate (Table IV). A common feature of all three complexes is that the phosphinyl oxygen–Zn distance on the electrophilic (His-231) side is shorter than that on the nucleophilic (Glu-143) side.

The transition states in the TLN- and CPA-catalyzed hydrolyses are presumed to have the *gem*-diolate oxygens of the tetrahedral carbon bound to zinc and the active-site electrophile

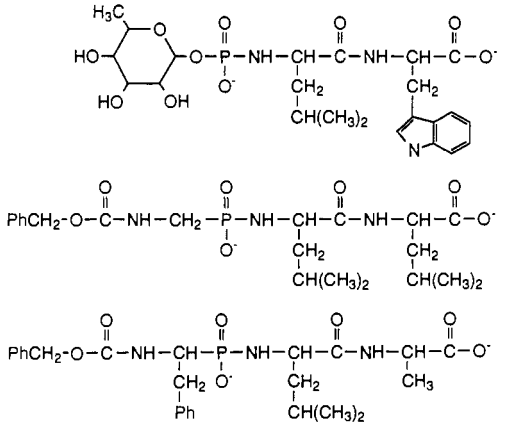

FIGURE 6: Three phosphinyl inhibitors of thermolysin. From top to bottom: *N*-[(α-L-rhamnopyranosyloxy)hydroxyphosphinyl]-L-Leu-L-Trp (phosphoramidon), K_i = 28 nM; (benzyloxycarbonyl)-Gly^P-L-Leu-L-Leu (ZG^{P}LL), K_i = 9.1 nM; (benzyloxycarbonyl)-Phe^P-L-Leu-L-Ala (ZF^{P}LA), K_i = 0.068 nM. ZG^{P}LL and ZF^{P}LA were shown to be transition-state analogues of the TLN-catalyzed hydrolysis (Bartlett & Marlowe, 1983, 1987a).

(His-231 in TLN, Arg-127 in CPA) in a progression of orientations that at some stages involves possible bidentate coordination to zinc (Monzingo & Matthews, 1984; Christianson & Lipscomb, 1988b). This bidentate coordination would represent a very effective charge interaction between the *gem*-diolate and the zinc, aided by the His-231 or Arg-127 interaction. In the complex of thermolysin with ZF^{P}LA, bidentate coordination of the phosphinyl oxygens to the zinc was taken as a strong confirmation of transition-state analogy. Bartlett had earlier demonstrated that these phosphonamidates were transition-state analogues of the TLN-catalyzed hydrolysis (Bartlett & Marlowe, 1983, 1987a). For the present case, coordination of the phosphinyl group of ZAA^P(O)F to the zinc strongly resembles that seen in the complexes of TLN with ZG^{P}LL and ZF^{P}LA (Figure 7; Table IV). The Zn–phosphinyl oxygen distances are 2.2 and 3.1 Å, respectively, for the electrophilic and nucleophilic sides. The important feature is that, like the TLN–phosphonamidate complexes, the CPA-ZAA^P(O)F complex has the phosphinyl moiety of the inhibitor rotated toward the electrophilic active-site residue. This similarity in the transition-state-analogue binding modes between CPA and TLN may indicate a similarity in their hydrolytic mechanisms.

It remains to be seen whether or not even tighter binding phosphonate inhibitors of CPA will coordinate to the zinc in

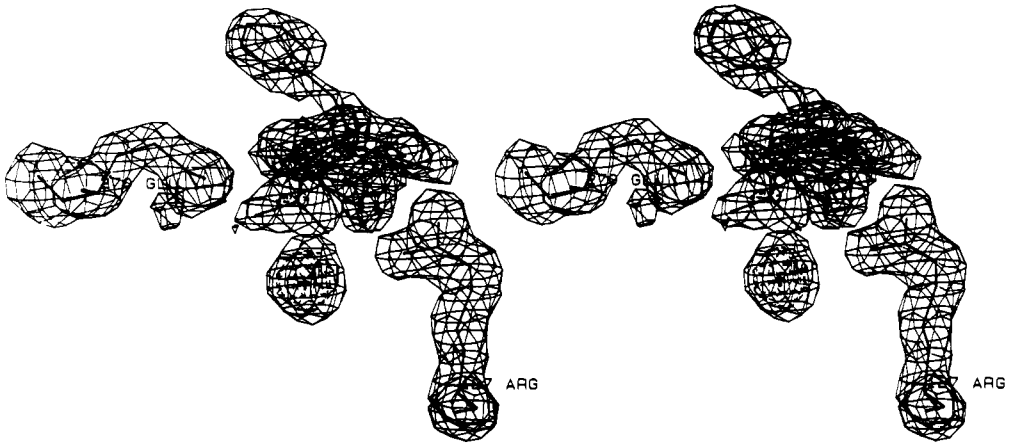

FIGURE 7: Interaction of the phosphinyl group with the zinc and the active-site nucleophile (Glu-270) and electrophile (Arg-127). The density drawn in lines is an $F_o - F_c$ map made with ZAA^P(O)F, the zinc, Glu-270, and Arg-127 omitted from the structure factor calculation. The contour level is 3σ. The stippled density is the same map contoured at 12σ to show the refined position of the zinc and phosphorus.

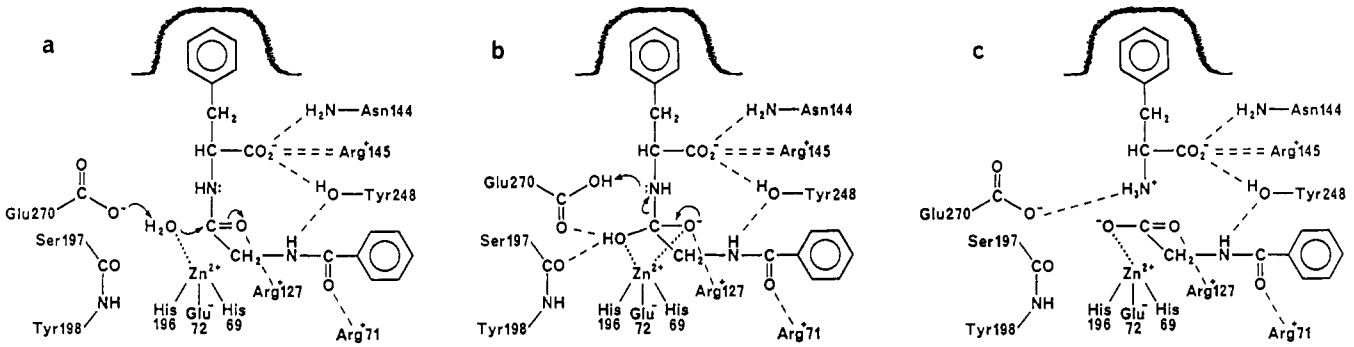

FIGURE 8: Proposed mechanism for CPA-catalyzed proteolysis: (a) the precatalytic Michaelis complex with the substrate carbonyl hydrogen bonded to Arg-127 allows for nucleophilic attack by a water molecule promoted by zinc and assisted by Glu-270; (b) the stabilized tetrahedral intermediate collapses with required proton donation by Glu-270; (c) the final product complex, after a second and final proton transfer mediated by Glu-270. Reproduced with permission from Christianson and Lipscomb (1989). Copyright 1989 American Chemical Society.

a nearly bidentate fashion as was seen for the TLN-ZF^{P}LA structure. Although a bidentate coordination of the transition-state *gem*-diolate is proposed for the transition states of both the CPA- and TLN-catalyzed hydrolyses, such a bidentate transition-state analogue may not be realized with phosphinyl inhibitors, as tight binding as they may be. Christianson and co-workers reported that the symmetrical bidentate phosphinyl–metal interaction is unfavorable due to electronic limitations (Alexander et al., 1990). Indeed, the 0.4-Å asymmetry of the phosphinyl oxygen–Zn coordination seen in the TLN-ZF^{P}LA structure (Holden et al., 1987) may be an approximate limit of the aproach toward equality of these Zn–O distances.

The phosphinyl oxygen–electrophile and –nucleophile distances in the present complex are also similar to those in the TLN–phosphonamidate complexes. Most notable are the very close phosphinyl oxygen–nucleophile distances. Carboxyl oxygens are known to make very close contacts, with oxygen–oxygen distances as close as 2.4 Å (Jeffrey & Maluszynska, 1982). Such a close oxygen–oxygen interaction in the present complex strongly suggests that one of the oxygens is protonated. The protonated oxygen is probably the glutamate oxygen since the pK_a of the phosphonate group (3.0) is likely lower than that of the glutamate side chain (4.5) (Freedman & Doak, 1957; Kam et al., 1979). A protonated glutamate fits nicely into the scheme of the general-base mechanism (Figure 8; Christianson & Lipscomb, 1989; Monzingo & Matthews, 1984; Jacobsen & Bartlett, 1981). By abstracting a hydrogen from the active-site water and thereby protonating itself, the glutamate (along with the zinc) activates the water for nucleophilic attack on the scissile carbon. In model compounds, Zn-bound waters such as the one in the active site of native CPA are shown to be quite nucleophilic, having pK_a's as low as 7 (Groves & Olson, 1985). In the present complex, the refinement program tended to push the phosphinyl group away from Glu-270, most likely to alleviate the close contact between the phosphinyl and glutamate oxygen, but this produced a structure for the inhibitor that did not fit well into the electron density maps. This problem was remedied by disabling the van der Waals and electrostatic energy terms of the refinement program, which kept the inhibitor well positioned in its density and yet maintained reasonable interatomic distances.

The present study, which emphasizes the general-base mechanism for CPA-catalyzed hydrolysis, need not dismiss the acyl mechanism, especially for certain substrates. Possible evidence supporting the acyl pathway for some substrates, e.g., cinnamoyl esters, has been reviewed by Christianson and Lipscomb (1989).

Kinetics of Binding. The cis carbamoyl ester bond in the bound ZAA^P(O)F is unusual (Figure 5). Ab initio calculations done in this laboratory at the Hartree–Fock 4-31G level on the prototypical carbamoyl ester, methyl carbamate, show that the trans conformation is more stable than the cis conformation by 1.6 kcal/mol, indicating that about 7% of a population of methyl carbamate would be in the cis conformation at room temperature (Liang, 1989). For the prototypical peptide molecule *N*-methylacetamide, ab initio studies at the Hartree–Fock 4-31G level indicate that the trans conformation of its peptide bond is 4.7 kcal/mol more stable than the cis

conformation (Ramani & Russell, 1981). According to this energy difference, less than 0.04% of a population of *N*-methylacetamide molecules are in the cis conformation at room temperature. These results for *N*-methylacetamide and methyl carbamate are gas-phase calculations. Jorgensen and Gao have calculated the energetics of the cis and trans conformations of *N*-methylacetamide at a high level of theory for both the gas phase and in solution (Jorgensen & Gao, 1988). They calculated the free energy of the trans conformation to be 2.5 kcal/mol lower than that of the cis conformation in the gas phase. This result was essentially unchanged for *N*-methylacetamide in aqueous solution. Similar results are expected for methyl carbamate, most notably, the decrease in the cis vs trans energy difference at higher levels of theory.

The question remains concerning what is responsible for the cis conformation of the carbamoyl ester bond in the bound $ZAA^P(O)F$. Although no crystal structure is available for $ZAA^P(O)F$ itself, it most likely exists in solution with its carbamoyl ester bond in the more stable trans conformation. If $ZAA^P(O)F$ is modeled into the active site with its carbamoyl ester bond in the trans conformation, the carbonyl and benzyl oxygen atoms of the Cbz portion still do not make any hydrogen bond contacts to the enzyme and the accompanying edge-to-face interaction between the phenyl ring of the Cbz group and the side chain of Tyr-198 is lost. Also, the trans conformation of this bond brings the Cbz portion of the inhibitor into unfavorably close contact with a symmetry-related complex in the crystal. Are crystal-packing forces then responsible for the cis conformation of the carbamoyl ester bond? If the inhibitor had been soaked into the enzyme crystals, then it is plausible that the inhibitor may have conformed to a binding mode dictated by steric factors due to preexisting symmetry-related molecules. However, our crystals were obtained through cocrystallization of the enzyme–inhibitor complex from solution. It therefore seems most probable to us that the molecular conformations of the complex seen in the crystal structure are those that exist in solution. If the inhibitor had indeed bound to the enzyme with a trans carbamoyl ester bond, the complex most likely would have crystallized in a different crystal structure such that there would have been no unfavorable crowding between the Cbz portion and a symmetry-related complex. Because the electron density in this region is as prominent as that for any other portion of the inhibitor, local disorder does not occur and the assignment of the cis conformation is unambiguous. One explanation for the cis carbamoyl ester bond appears to be that the stabilization afforded by the edge-to-face interaction of aromatic rings in this region is greater than the energy difference between the trans and cis conformations of the carbamoyl ester bond.

Studies by Bartlett's group on this series of phosphonate inhibitors of CPA showed that k_{on} for $ZAG^P(O)F$ was higher than that of inhibitors with an α-substituted P_1 residue. For $ZAA^P(O)F$, $k_{on} = 2.1 \times 10^5\ M^{-1}\ s^{-1}$ and for $ZAG^P(O)F$, $k_{on} = 6.6 \times 10^5\ M^{-1}\ s^{-1}$ (Hanson et al., 1989). This glycyl vs α-substiuted k_{on} result was also seen in a series of phosphonamidate inhibitors of thermolysin (Bartlett & Marlowe, 1987a). For the thermolysin inhibitors, it has been speculated that the slower k_{on} for the α-substituted inhibitor may be due to hindered dissociation of a water molecule that occupies a binding site in the native enzyme (Holden et al., 1987; Bartlett & Marlowe, 1987a). The α-substituted inhibitor may have to expel this water in order to accommodate its binding mode whereas the P_1 glycyl inhibitor, with its greater conformational freedom, can adopt a binding mode that does not require the expulsion of the water molecule. For the phosphonate CPA inhibitors, this k_{on} result may be due to the interconversion of the carbamoyl ester bond from trans in solution to cis in the bound state. The presence of glycine at the P_1 position would give the inhibitor more conformational freedom, thereby making possible a binding mode that may not require the energetically costly conversion to a cis carbamoyl ester bond. Alternatively, the enzyme may selectively bind those molecules of $ZAA^P(O)F$ that already exist in solution with a cis carbamoyl ester linkage. Thus, for both scenarios, the binding of the α-substituted inhibitor would depend on the slow trans to cis interconversion of the carbamoyl ester linkage, either in a collision complex or in solution.

Comparison with Phosphonamidate Binding. The type of phosphinyl–Zn coordination described earlier is different from that seen in the complex of CPA with the phosphonamidate inhibitor ZGP′, an analogue of Cbz-Gly-L-Phe (Christianson & Lipscomb, 1988b). In that complex, the phosphinyl moiety was rotated toward the active-site nucleophile (Table IV). This orientation should not discredit the comparison that has been made between the present complex and the TLN–phosphonamidate complexes. ZGP′ is a dipeptide analogue with $Cbz\text{-}Gly^P$ at the protecting group P_1 position. Dipeptide ligands of CPA with glycine in the P_1 position exhibit structural and kinetic anomalies. In the CPA–ZGP′ complex, the Cbz-Gly portion of the inhibitor occupied the S_1 hydrophobic pocket and the complex of CPA with the ketonic analogue of benzoyl-Gly-L-Phe showed the benzamido moiety to be disordered (Christianson et al., 1987). Kinetic anomalies have been observed for Cbz-Gly-L-Phe and other similar dipeptide substrates (Davies et al., 1968; Auld & Vallee, 1970) and the behavior of ZGP′ does not fit simple competitive, noncompetitive, or mixed inhibition (Jacobsen & Bartlett, 1981). In light of these anomalies, it is not surprising that the CPA–phosphonamidate complex shows a phosphinyl coordination different from that seen in the present complex and the TLN–phosphonamidate complexes. Dipeptide inhibitors with glycine in the P_1 position may only be good models for the binding of their analogous CPA substrates and may be much less effective in mimicking the binding of more extended or P_1-substituted substrates.

A significant difference between $ZAA^P(O)F$ and ZGP′ is in their respective binding constants, 3 pM (Hanson et al., 1989) and 90 nM (Jacobsen & Bartlett, 1981). Certainly, one of the reasons for the 4 orders of magnitude tighter binding for $ZAA^P(O)F$ is that $ZAA^P(O)F$ is a more extended ligand and is therefore able to make more contacts to the enzyme in the active site. Most notable is the hydrogen bond of the S_2 subsite involving Arg-71. Small differences in enzyme–inhibitor contacts between two complexes can account for large changes in the strength of binding. For TLN, the phosphonamidate analogue of Cbz-Gly-L-Leu-L-Leu binds by nearly 3 orders of magnitude more tightly than the analogous phosphonate (Bartlett & Marlowe, 1983, 1987b). Structural studies of the complexes of TLN with these two phosphinyl inhibitors show that the two binding modes are virtually identical and that the difference in binding constants for the two inhibitors is attributable to the presence or absence of a single hydrogen-bonding group (Tronrud et al., 1987; Bartlett & Marlowe, 1987b). Another explanation for the difference in binding constants between $ZAA^P(O)F$ and ZGP′ comes from, once again, transition-state-binding theory. Data from solution studies supporting the transition-state analogy for $ZAA^P(O)F$ is much clearer than that for ZGP′ (Hanson et al., 1989; Jacobsen & Bartlett, 1981). The apparent difference

in transition-state analogy for these two inhibitors may lie in subtle changes in their binding modes, such as the orientation of the phosphinyl group. The actual tetrahedral transition state of the general-base mechanism may be better modeled by the rotation of the phosphinyl group toward the electrophilic active-site residue, as in the tighter binding $ZAA^{P}(O)F$, rather than toward the nucleophilic active-site residue.

ACKNOWLEDGMENTS

We gratefully acknowledge Prof. P. A. Bartlett for providing $ZAA^{P}(O)F$. We thank Dr. H. Zemel for helpful discussions concerning the mechanism of the CPA-catalyzed hydrolysis and Dr. J. Y. Liang for the calculations on methyl carbamate. Profs. P. A. Bartlett and D. W. Christianson and Drs. J. E. Gouaux and R. C. Stevens are acknowledged for their insightful comments on the manuscript. H.K. thanks Drs. J. E. Hanson and S. Subbiah for excellent discussions.

REFERENCES

Abramowitz, N., Schechter, I., & Berger, A. (1967) *Biochem. Biophys. Res. Commun. 29*, 862–867.

Alexander, R. S., Kanyo, Z. F., Chirlian, L. E., & Christianson, D. W. (1990) *J. Am. Chem. Soc. 112*, 933–937.

Auld, D. S., & Vallee, B. L. (1970) *Biochemistry 9*, 602–609.

Bartlett, P. A., & Marlowe, C. K. (1983) *Biochemistry 22*, 4618–4624.

Bartlett, P. A., & Marlowe, C. K. (1987a) *Biochemistry 26*, 8553–8561.

Bartlett, P. A., & Marlowe, C. K. (1987b) *Science 235*, 569–571.

Brünger, A. T. (1988) *X-PLOR Manual*, Version 1.5.

Brünger, A. T., Kuriyan, J., & Karplus, M. (1987) *Science 235*, 458–460.

Burley, S. K., & Petsko, G. A. (1985) *Science 229*, 23–28.

Burley, S. K., & Petsko, G. A. (1986) *J. Am. Chem. Soc. 108*, 7995–8001.

Christianson, D. W., & Lipscomb, W. N. (1985) *Proc. Natl. Acad. Sci. U.S.A. 82*, 6840–6844.

Christianson, D. W., & Lipscomb, W. N. (1986) *J. Am. Chem. Soc. 108*, 4998–5003.

Christianson, D. W., & Lipscomb, W. N. (1988a) *Colloq. Ges. Biol. Chem., 39th*, 65–74.

Christianson, D. W., & Lipscomb, W. N. (1988b) *J. Am. Chem. Soc. 110*, 5560–5565.

Christianson, D. W., & Lipscomb, W. N. (1989) *Acc. Chem. Res. 22*, 62–69.

Christianson, D. W., David, P. R., & Lipscomb, W. N. (1987) *Proc. Natl. Acad. Sci. U.S.A. 84*, 1512–1515.

Davies, R. C., Riordan, J. F., Auld, D. S., & Vallee, B. L. (1968) *Biochemistry 7*, 1090–1099.

Freedman, L. D., & Doak, G. O. (1957) *Chem. Rev. 57*, 479–523.

Galardy, R. E., & Kortylewicz, Z. P. (1984) *Biochemistry 23*, 2083–2087.

Gelb, M. H., Svaren, J. P., & Abeles, R. H. (1985) *Biochemistry 24*, 1813–1817.

Grobelny, D., Goli, U. B., & Galardy, R. E. (1985) *Biochemistry 24*, 7612–7617.

Groves, J. T., & Olson, J. R. (1985) *Inorg. Chem. 24*, 2715–2717.

Hanson, J. E., Kaplan, A. P., & Bartlett, P. A. (1989) *Biochemistry 28*, 6294–6305.

Holden, H. M., Tronurd, D. E., Monzingo, A. F., Weaver, L. H., & Matthews, B. W. (1987) *Biochemistry 26*, 8542–8553.

Holmes, M. A., & Matthews, B. W. (1982) *J. Mol. Biol. 160*, 623–639.

Jacobsen, N. E., & Bartlett, P. A. (1981) *J. Am. Chem. Soc. 103*, 654–657.

Jeffrey, G. A., & Maluszynska, H. (1982) *Int. J. Biol. Macromol. 4*, 173–185.

Jones, T. A. (1982) in *Computational Crystallography* (Sayre, D., Ed.) pp 303–317, Clarendon Press, Oxford.

Kaiser, B. L., & Kaiser, E. T. (1969) *Proc. Natl. Acad. Sci. U.S.A. 64*, 36–41.

Kam, C.-M., Nishino, N., & Powers, J. C. (1979) *Biochemistry 18*, 3032–3038.

Leinhard, G. E. (1973) *Science 180*, 149–154.

Liang, J. Y. (1989) (unpublished result).

Machin, P. A. (1985) *Daresbury Lab. [Rep.] DL/SCI/R23.*

Matthews, B. W. (1988) *Acc. Chem. Res. 21*, 333–340.

Monzingo, A. F., & Matthews, B. W. (1984) *Biochemistry 23*, 5724–5729.

Pauling, L. (1948) *Nature 161*, 707–709.

Quiocho, F. A., & Lipscomb, W. N. (1971) *Adv. Protein Chem. 25*, 1–78.

Ramani, R., & Russell, J. B. (1981) *Int. J. Quant. Chem., Quant. Biol. Symp. 8*, 117–127.

Reeke, G. N., Hartsuck, J. A., Ludwig, M. L., Quiocho, F. A., Steitz, T. A., & Lipscomb, W. N. (1967) *Proc. Natl. Acad. Sci. U.S.A. 58*, 2220–2226.

Rees, D. C., & Lipscomb, W. N. (1982) *J. Mol. Biol. 160*, 475–498.

Rees, D. C., Lewis, M., & Lipscomb, W. N. (1983) *J. Mol. Biol. 168*, 367–387.

Shoham, G., Christianson, D. W., & Oren, D. A. (1988) *Proc. Natl. Acad. Sci. U.S.A. 85*, 684–688.

Thompson, R. C. (1973) *Biochemistry 12*, 47–51.

Tronrud, D. E., Monzingo, A. F., & Matthews, B. W. (1986) *Eur. J. Biochem. 157*, 261–268.

Tronrud, D. E., Holden, H. M., & Matthews, B. W. (1987) *Science 235*, 571–574.

Wolfenden, R. (1976) *Annu. Rev. Biochem. Bioeng. 5*, 271–306.